THE JOURNAL OF PHYSICAL CHEMISTRY LETTERS
A JOURNAL OF THE AMERICAN CHEMICAL SOCIETY

pubs.acs.org/JPCL

Letter

Optical Fingerprint Classification of Single Upconversion Nanoparticles by Deep Learning

Jiayan Liao, Jiajia Zhou,* Yiliao Song, Baolei Liu, Jie Lu, and Dayong Jin

Cite This: *J. Phys. Chem. Lett.* 2021, 12, 10242−10248

Read Online

ACCESS | Metrics & More | Article Recommendations | Supporting Information

ABSTRACT: Highly controlled synthesis of upconversion nanoparticles (UCNPs) can be achieved in the heterogeneous design, so that a library of optical properties can be arbitrarily produced by depositing multiple lanthanide ions. Such a control offers the potential in creating nanoscale barcodes carrying high-capacity information. With the increasing creation of optical information, it poses more challenges in decoding them in an accurate, high-throughput, and speedy fashion. Here, we reported that the deep-learning approach can recognize the complexity of the optical fingerprints from different UCNPs. Under a wide-field microscope, the lifetime profiles of hundreds of single nanoparticles can be collected at once, which offers a sufficient amount of data to develop deep-learning algorithms. We demonstrated that high accuracies of over 90% can be achieved in classifying 14 kinds of UCNPs. This work suggests new opportunities in handling the diverse properties of nanoscale optical barcodes toward the establishment of vast luminescent information carriers.

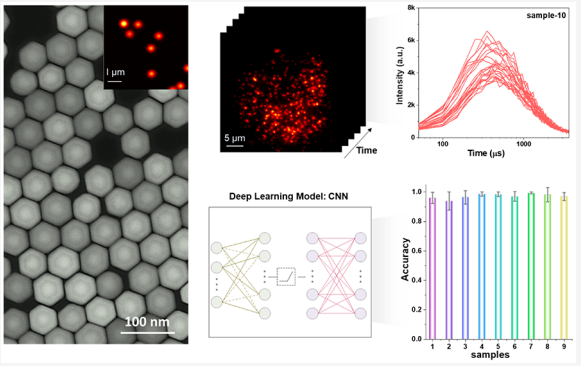

The development of new materials' encoding strategies has extended our capacity to acquire, store, and process information. The ongoing development of optical multiplexing technologies involves organic (fluorescent dyes)[1−4] and inorganic fluorophores (quantum dots,[5−8] carbon dot,[9,10] and lanthanide-doped nanoparticles[11−15]) as optical information carriers. Their emissive features in the spectral domain can be used in multiplexed assays, imaging, and tracking of biomolecules *in vitro* and *in vivo*.[16] This has been achieved typically by mixing the varied ratios of a fluorescence nanomaterial, such as multicolor quantum dots,[17,18] or lanthanide-doped nanoparticles,[19,20] and encapsulating them into microsphere beads.

While color encoding is limited by the spectrum cross-talk issue, the recent development of time-domain optical carriers provides a new opportunity for high-capacity multiplexing by adding transient information on emissions.[21−25] Lanthanide-doped upconversion nanoparticles (UCNPs) with sharp emission spectra, long lifetimes, and exceptional nonblinking and nonbleaching photostability[26] are particularly suitable for this purpose. UCNPs have been applied in high-throughput bioassays, imaging of cellular molecules' transport, anticounterfeiting security inks, and data storage.[27,28] Encapsulation of the Yb^{3+}-Tm^{3+}-doped UCNPs has been demonstrated to encode suspension arrays of microspheres, which can be time-resolved on a stage scanning microscope.[29] The Nd^{3+}-Yb^{3+}-Er^{3+}-tridoped core/multishell UCNPs have been used in polystyrene microspheres, which extends the encoding capacity by both luminescence colors and decay lifetimes.[20]

Toward the desirable nanoscale multiplexing, we recently demonstrated a highly controlled synthesis of heterogeneous UCNPs, which allows time-domain tuning of their emission properties to create a large set of lifetime fingerprints.[30] We exemplified that the three dimensions of excitation wavelength, emission color, and lifetime profile (named as τ^2, as both the rising and decay time features are involved) can be used to produce a vast library of nanotags, toward the applications in data storage, security inks, single-molecule digital assay, and super-resolution imaging.[30] In the time-domain dimension, the entire lifetime profile can be used to encode UCNPs. But we conclude that conventional data analytics approaches are tedious and insufficient in extracting all the features from the time-domain profiles of UCNPs.

The recent surge of machine learning approaches has been found useful in guiding the synthesis and modeling,[31−36] as well as classifying, predicting, and discovering new materials.[37−43] Machine learning algorithms based on the chemical reaction data have been used to predict the formation conditions for vanadium selenite crystallization of metal−organic framework materials with a success rate of 89%.[40] The ability of deep

Received: September 5, 2021
Accepted: October 11, 2021
Published: October 14, 2021

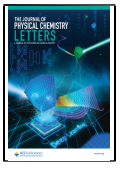

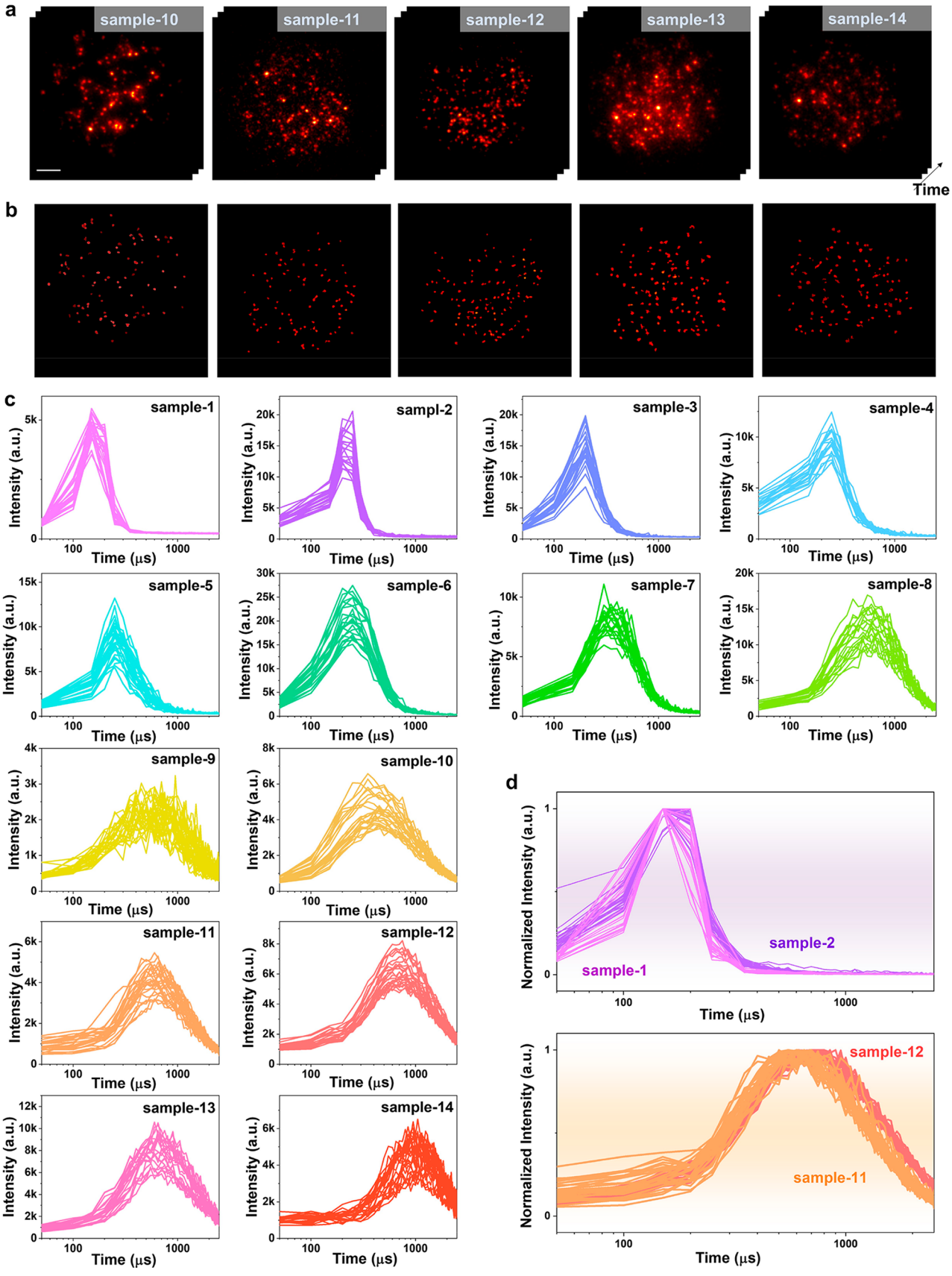

Figure 1. Lifetime profiles of single UCNPs under time-resolved wide-field microscopy. (a) Peak moment images (the brightest frame) were selected from the series of time-resolved images. The 808 nm laser excitation pulse of 200 μs is used. (b) Corresponding images of part a after selecting the single nanoparticles. (c) Lifetime profiles of the typical 20 single UCNPs extracted from the time-resolved image series of sample-1 to -14. (d) Similarity in the lifetime profiles of single UCNPs between sample-1 and sample-2 and between sample-11 and sample-12. Scale bar: 5 μm.

https://doi.org/10.1021/acs.jpclett.1c02923
J. Phys. Chem. Lett. 2021, 12, 10242−10248

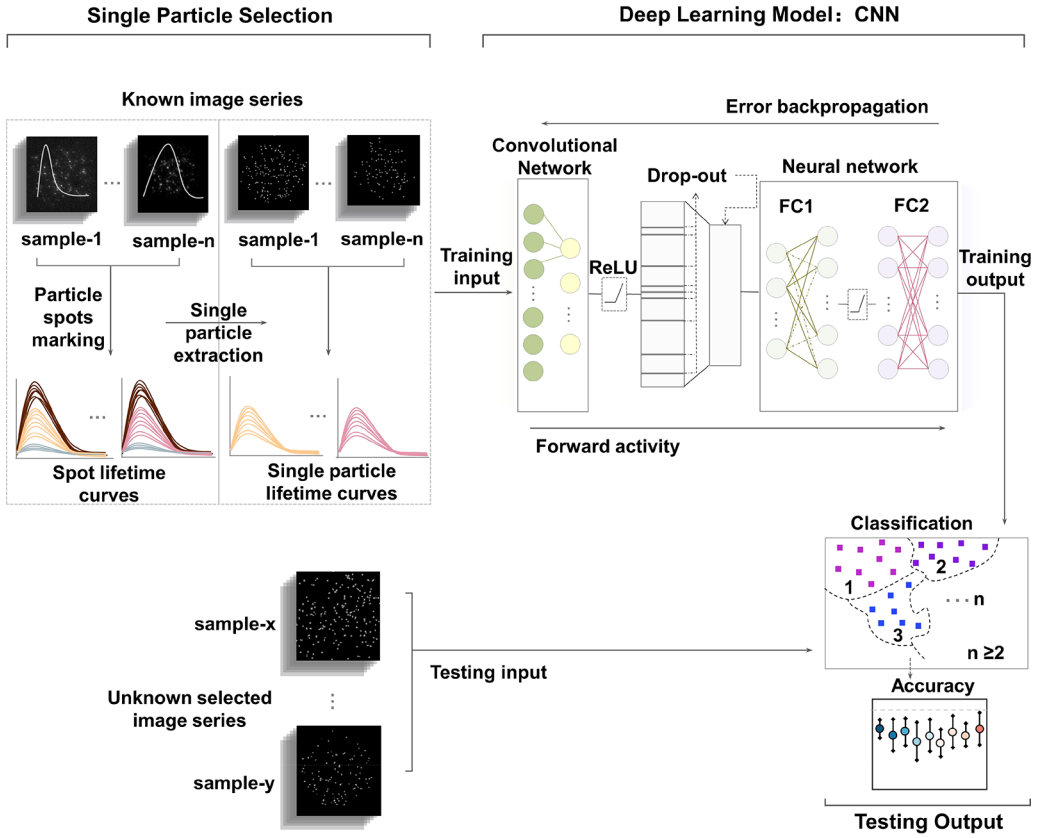

Figure 2. Data processing and deep learning framework for recognizing the lifetime fingerprint of single UCNPs. The as-collected images were first preprocessed by selecting the single nanoparticles. Then the artificial neural network extracts the curve features of each type of UCNPs and provides the optimized CNN and classification boundaries by getting feedback from accuracies.

learning approaches has been shown in recognition and classification of the highly nonlinear data sets[44] and the curve features from optical materials by using an artificial neural network.[45,46]

Here, we evaluate the classification of the lifetime profiles among different batches of UCNPs using a deep learning algorithm. This is achieved by the time-resolved imaging of single UCNPs to generate the data set of lifetime fingerprints. We show that deep learning can intelligently define a territory for each type of 14 batches of UCNPs with accuracies higher than 90% achieved. This work suggests the potentials in handling the growing amount of optical information to build a nanoscale material library for supercapacity multiplexing applications.

Here two series of nine batches of Yb^{3+}-Tm^{3+}-codoped and five batches of Nd^{3+}-Yb^{3+}-Er^{3+}-tridoped UCNPs were investigated. The morphological and optical characterization results are provided in Table S1 and Figures S1−S6. We employ a wide-field microscope system to achieve high-throughput data collection (Figure S7). Compared to the point-by-point scanning approach, the wide-field microscope can simultaneously collect the lifetime profiles from hundreds of single nanoparticles from each measurement. The exceptional optical stability of single UCNPs affords these nanoparticles with continuous imaging for more than 250 min (see Figure S8). The sequence of 75 consecutive frames of time-resolved images with the time-gated window of 50 μs was collected by an intensifier coupled CMOS camera.

Figure 1a shows the typical time-gated images at the intensity peak for 50 μs, from the series of time-resolved images, which show hundreds of Nd^{3+}-Yb^{3+}-Er^{3+}-codoped UCNPs from each batch of the synthesis. As the unavoidable aggregates may exist in the imaging field of view, we selected the single nanocrystals by performing the OTSU data processing algorithm (see Materials and Methods in the Supporting Information). Figure 1b is the corresponding selected single-particle images of Figure 1a, each containing ~90 single nanoparticles. The typical lifetime profiles of the typical 20 single UCNPs are displayed in Figure 1c, representing the data collected from the samples from batch-1 to batch-14. The variations of the emission intensities are due to the uneven Gaussian distribution of the excitation laser and the nonlinear power dependence of the upconversion emission behavior.[30] The collected signals of each time-domain fingerprint are also noisy, due to the limited photons that can be collected within each 50 μs time-gated window. To facilitate the data analysis, all the lifetime profiles have been normalized at the lifetime peak moment. Notably, Figure 1d shows the typical challenge in differentiating the highly overlapped lifetime profiles from any two batches of UCNPs.

The deep learning algorithm, based on an architecture of convolutional neural networks (CNN), was implemented to define the classification boundaries of the lifetime fingerprints of the 14 batches of UCNPs. Figure 2 illustrates the deep learning-aided decoding process. A deep learning package Pytorch was used to train the image series and validate and test the neural network. Before classifying the time-domain single nanoparticles, the network architecture of deep learning was established (Supporting Information section 4). The decreasing categorical cross-entropy loss curves in Figure S9 show that all the hyper-parameters were well-optimized after adjusting the

https://doi.org/10.1021/acs.jpclett.1c02923
J. Phys. Chem. Lett. 2021, 12, 10242−10248

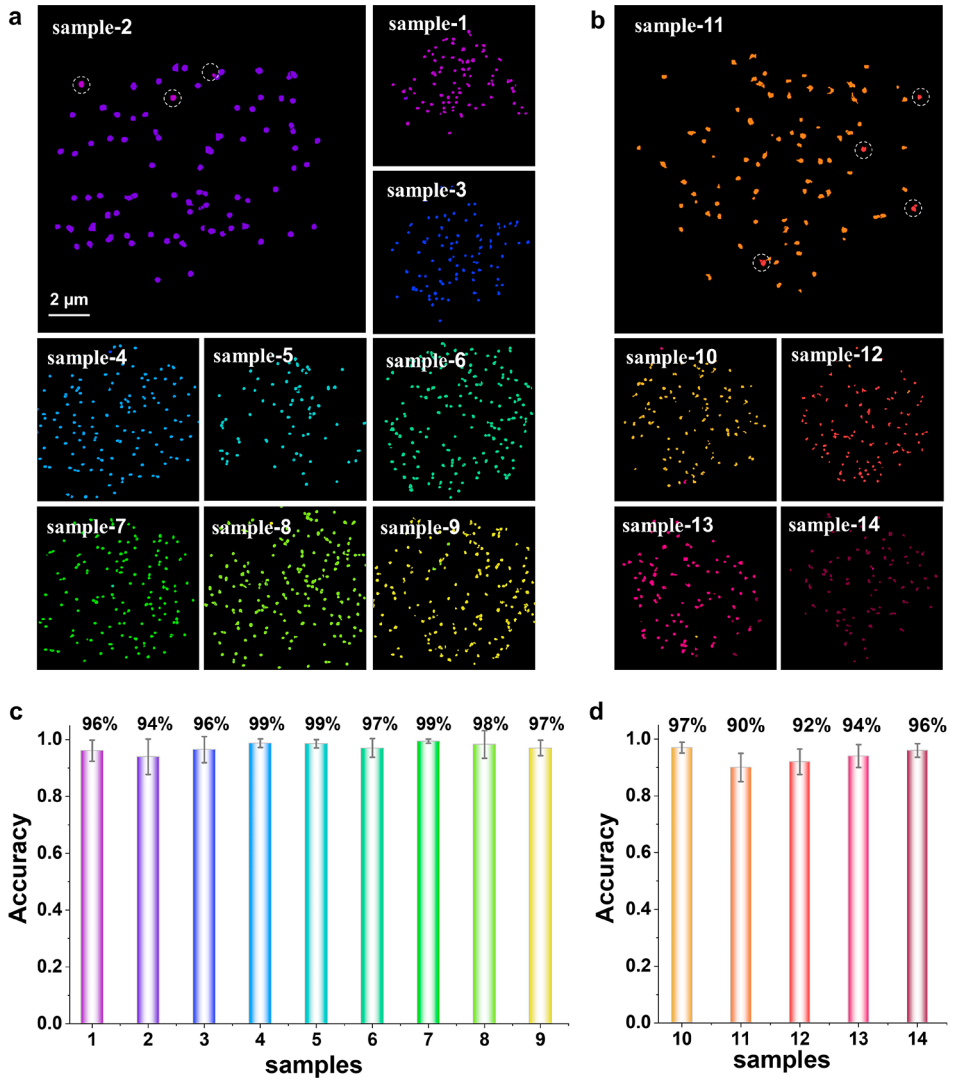

Figure 3. Deep learning aided decoding of lifetime fingerprints of single UCNPs. (a and b) One set of classification result images for the Yb−Tm series UCNP from sample-1 to sample-9 UCNPs (a) and Nd−Yb−Er series UCNPs from sample-10 to sample-14 UCNPs (b). For the visualization purpose, pseudocolor is used to represent each type of single UCNPs. (c and d) Mean classification accuracy was obtained through the cross-validation experiment.

key aspects to establish the networking architecture. We employed the optimum network structure, which consists of two convolutional networks followed by two fully connected networks (FC1 and FC2) to define the feature coverage and the classification boundaries for each batch of UCNPs. The two 1D convolutional layers used the element-wise function $ReLU6(x) = \min(\max(0, x), 6)$. The hyper-parameters of the network were optimized by choosing the highest average accuracy of the validation curves of the number of neurons (Figures S10 and S11), the dropout rate (Figure S12), the batch size (Figure S13), and the learning rate (Figure S14). After the network structure was determined, we verified the deep learning algorithm by randomly selecting a set of unused lifetime profiles from the two series of the 14 batches of UCNPs, e.g., the sample-1 to -9 of Yb^{3+}-Tm^{3+}-doped UCNPs and sample-10 to -14 of Nd^{3+}-Yb^{3+}-Er^{3+}-doped UCNPs.

We first collected seven sets of time-resolved sequences of images from each batch of UCNP samples, each of which contains the lifetime fingerprints of ∼600 single nanoparticles. We randomly used the first six sets of imaging data from each batch of UCNPs to train the machine to establish a neural network, with the remaining set of data used as validation analytes. After one training-and-testing process, the testing error for the 14 image sequences was obtained. To eliminate the random effect, we repeated the cross-validation experiment 50 times, in which ∼500 single nanoparticles of each type were randomly selected for testing and the remaining 100 were used for training. The mean classification accuracy and deviation of errors for each type of UCNPs were computed through these 50 random experiments.

For visualizing the classification result, we marked each type of single UCNPs with a pseudocolor. One representative set of results from sample-1 to sample-9 and sample-10 to sample-14 is displayed in Figure 3a and b. The statistical distributions of classification accuracy with error bars by running the experiment of training and validation 50 times are displayed in Figure 3c and d. We achieved the mean classification accuracies for each UCNP sample with all the values reaching over 90%. Tables S2 (Yb^{3+}-Tm^{3+}-doped UCNPs) and S3 (Nd^{3+}-Yb^{3+}-Er^{3+}-doped UCNPs) show the high classification accuracy between two samples over 20-trials under different neurons per FC layers. Their classification accuracies are hovering over the range 91%−

https://doi.org/10.1021/acs.jpclett.1c02923
J. Phys. Chem. Lett. 2021, 12, 10242−10248

100%. The small number of dots with mismatched colors represent the error recognition (e.g., there are some misrecognition dots of sample-1 in the image of sample-2, and sample-12 in the image of sample-11), which is mainly caused by the unavoidable noise background (consistent with the curves in Figure 1d).

We highlight that the brightness of single nanoparticles is important to ensure the data quality for high recognition accuracy. For the nanoparticles of less brightness (see new sample-15, which has a half intensity decrease compared to the brightest sample-13 in Figure S15a), the relatively large variation in the lifetime profiles appeared from the same batch (Figure S15b). Therefore, less accurate classification can be achieved. Once a batch of the less bright nanoparticles is added into the library, adding another batch of bright sample-16 does not help to compensate for the low overall accuracy (Figure S15c). Moreover, even well-trained machine learning models may contain unavoidable errors due to the noise in the training data and measurement limitations. Therefore, strategies around synthesizing bright nanoparticles and improving the measurement efficiency under the limited budget of detectable photons are still needed to facilitate the deep learning approaches to be used in classifications of the lifetime profiles of single UCNPs for nanoscale optical multiplexing applications.

Through the use of time-resolved wide-field microscopy, we have achieved the high-throughput collection of the complex lifetime profiles of single UCNPs from multiple batches of controlled synthesis. These provide sufficient data sets for the deep learning algorithm development to classify the difference in the optical fingerprints among the multiple batches of UCNPs. We achieved in this work accuracies over 90%. The controlled synthesis of bright and optically stable single nanoparticles with characteristic lifetime fingerprints provides an untapped opportunity for nanoscale optical multiplexing. A deep learning algorithm provides a powerful way to assist the accurate decoding of nanoscale objects. This work further suggests that future synthesis of bright and uniform nanoparticles with tunable optical properties at single-particle level can be used to produce the optical fingerprints from the multiple optical dimensions, e.g., spectrum, lifetime, polarization, and intensity, and uses them to expand the current library of nanoparticle barcodes for supercapacity optical multiplexing. Assignments of these uniform and bright optical information carriers in nanoscale with the unique and distinguishable optical signatures will expand the analytical technology capacities and accelerate high-throughput biomolecular discoveries.

■ ASSOCIATED CONTENT

Supporting Information

The Supporting Information is available free of charge at https://pubs.acs.org/doi/10.1021/acs.jpclett.1c02923.

Details about material synthesis and characterization, optical systems setup, networks of deep learning, and experimental methods. Table S1: compositions of nanoparticles. Figures S1−S6: materials characterization. Figures S7 and S8: optical characterization. Figures S9−S15 and Tables S2 and S3: network architecture and results of deep learning (PDF)

■ AUTHOR INFORMATION

Corresponding Author

Jiajia Zhou − *Institute for Biomedical Materials and Devices (IBMD), Faculty of Science, University of Technology Sydney, NSW 2007, Australia;* orcid.org/0000-0002-0605-5745; Email: jiajia.zhou@uts.edu.au

Authors

Jiayan Liao − *Institute for Biomedical Materials and Devices (IBMD), Faculty of Science, University of Technology Sydney, NSW 2007, Australia;* orcid.org/0000-0002-0902-5381

Yiliao Song − *Australian Artificial Intelligence Institute, University of Technology Sydney, Sydney, New South Wales 2007, Australia*

Baolei Liu − *Institute for Biomedical Materials and Devices (IBMD), Faculty of Science, University of Technology Sydney, NSW 2007, Australia;* orcid.org/0000-0002-4779-4683

Jie Lu − *Australian Artificial Intelligence Institute, University of Technology Sydney, Sydney, New South Wales 2007, Australia*

Dayong Jin − *Institute for Biomedical Materials and Devices (IBMD), Faculty of Science, University of Technology Sydney, NSW 2007, Australia; UTS-SUStech Joint Research Centre for Biomedical Materials & Devices, Department of Biomedical Engineering, Southern University of Science and Technology, Shenzhen 518055, China;* orcid.org/0000-0003-1046-2666

Complete contact information is available at: https://pubs.acs.org/10.1021/acs.jpclett.1c02923

Author Contributions

J.Z. and D.J. cosupervised the research. J.Z., D.J., and J.L. conceived the project and designed the experiments. J.L. conducted the synthesis, characterization, and measurement. J.L. and B.L. processed the data and built the optical system. Y.S. and J.Lu. conducted the machine learning experiment. J.L. and J.Z. prepared the figures and Supporting Information. J.L., J.Z., and D.J. wrote the manuscript with input from other authors.

Notes

The authors declare no competing financial interest.

■ ACKNOWLEDGMENTS

The authors acknowledge the financial support from the Australian Research Council Discovery Early Career Researcher Award Scheme (J.Z., DE180100669), Australian Research Council Laureate Fellowship Program (D.J., FL210100180 and J. Lu., FL190100149), China Scholarship Council Scholarships (Jiayan Liao: No. 201508530231, Baolei Liu: No. 201706020170), Australia-China Joint Research Centre for Point-of-Care Testing (ACSRF65827, 2017YFE0132300), Science and Technology Innovation Commission of Shenzhen (KQTD20170810110913065), National Natural Science Foundation of China (61729501), and the CAS/SAFEA International Partnership Program for Creative Research Teams and Major International (Regional) Joint Research Project of NSFC (51720105015).

■ REFERENCES

(1) Li, Y.; Cu, Y. T. H.; Luo, D. Multiplexed Detection of Pathogen DNA with DNA-Based Fluorescence Nanobarcodes. *Nat. Biotechnol.* **2005**, *23* (7), 885−889.

(2) Tong, A. K.; Li, Z.; Jones, G. S.; Russo, J. J.; Ju, J. Combinatorial Fluorescence Energy Transfer Tags for Multiplex Biological Assays. *Nat. Biotechnol.* **2001**, *19* (8), 756−759.

(3) Liu, X.; Bing, T.; Shangguan, D. Microbead-Based Platform for Multiplex Detection of DNA and Protein. *ACS Appl. Mater. Interfaces* **2017**, *9* (11), 9462−9469.
(4) Lei, Z.; Sun, C.; Pei, P.; Wang, S.; Li, D.; Zhang, X.; Zhang, F. Stable, Wavelength-Tunable Fluorescent Dyes in the NIR-II Region for In Vivo High-Contrast Bioimaging and Multiplexed Biosensing. *Angew. Chem.* **2019**, *131* (24), 8250−8255.
(5) Gai, H.; Liu, X.; Sun, Y.; Lin, X.; Pan, X.; Wu, Z. Digital Duplex Homogeneous Immunoassay by Counting Immunocomplex Labeled with Quantum Dots. *Anal. Chem.* **2021**, *93* (6), 3089−3095.
(6) Duan, H.; Li, Y.; Shao, Y.; Huang, X.; Xiong, Y. Multicolor Quantum Dot Nanobeads for Simultaneous Multiplex Immunochromatographic Detection of Mycotoxins in Maize. *Sens. Actuators, B* **2019**, *291*, 411−417.
(7) Qu, X.; Bian, F.; Guo, Q.; Ge, Q.; Sun, Q.; Huang, X. Ligation-Rolling Circle Amplification on Quantum Dot-Encoded Microbeads for Detection of Multiplex G-Quadruplex-Forming Sequences. *Anal. Chem.* **2018**, *90* (20), 12051−12058.
(8) Dehghani, A.; Ardekani, S. M.; Lesani, P.; Hassan, M.; Gomes, V. G. Two-Photon Active Boron Nitride Quantum Dots for Multiplexed Imaging, Intracellular Ferric Ion Biosensing, and Ph Tracking in Living Cells. *ACS Appl. Bio Mater.* **2018**, *1* (4), 975−984.
(9) Yu, X.; Liu, K.; Zhang, H.; Wang, B.; Yang, G.; Li, J.; Yu, J. Lifetime-Engineered Phosphorescent Carbon Dots-in-Zeolite Composites for Naked-Eye Visible Multiplexing. *CCS Chem.* **2021**, *3*, 252−264.
(10) Wang, S.; Kang, G.; Cui, F.; Zhang, Y. Dual-Color Graphene Quantum Dots and Carbon Nanoparticles Biosensing Platform Combined with Exonuclease III-Assisted Signal Amplification for Simultaneous Detection of Multiple DNA Targets. *Anal. Chim. Acta* **2021**, *1154*, 338346.
(11) Zhang, F.; Shi, Q.; Zhang, Y.; Shi, Y.; Ding, K.; Zhao, D.; Stucky, G. D. Fluorescence Upconversion Microbarcodes for Multiplexed Biological Detection: Nucleic Acid Encoding. *Adv. Mater.* **2011**, *23* (33), 3775−3779.
(12) Shikha, S.; Zheng, X.; Zhang, Y. Upconversion Nanoparticles-Encoded Hydrogel Microbeads-Based Multiplexed Protein Detection. *Nano-Micro Lett.* **2018**, *10* (2), 1−16.
(13) Farka, Z.; Mickert, M. J.; Hlaváček, A.; Skládal, P.; Gorris, H. H. Single Molecule Upconversion-Linked Immunosorbent Assay with Extended Dynamic Range for the Sensitive Detection of Diagnostic Biomarkers. *Anal. Chem.* **2017**, *89* (21), 11825−11830.
(14) Hu, L.; Fan, Y.; Liu, L.; Li, X.; Zhao, B.; Wang, R.; Wang, P.; El-Toni, A. M.; Zhang, F. Orthogonal Multiplexed Luminescence Encoding with Near-Infrared Rechargeable Upconverting Persistent Luminescence Composites. *Adv. Opt. Mater.* **2017**, *5* (22), 1700680.
(15) Liao, J.; Jin, D.; Chen, C.; Li, Y.; Zhou, J. Helix Shape Power-Dependent Properties of Single Upconversion Nanoparticles. *J. Phys. Chem. Lett.* **2020**, *11* (8), 2883−2890.
(16) Lin, G.; Baker, M. A. B.; Hong, M.; Jin, D. The Quest for Optical Multiplexing in Bio-Discoveries. *Chem.* **2018**, *4* (5), 997−1021.
(17) Yang, J.; Dave, S. R.; Gao, X. Quantum Dot Nanobarcodes: Epitaxial Assembly of Nanoparticle-Polymer Complexes in Homogeneous Solution. *J. Am. Chem. Soc.* **2008**, *130* (15), 5286−5292.
(18) Han, M.; Gao, X.; Su, J. Z.; Nie, S. Quantum-Dot-Tagged Microbeads for Multiplexed Optical Coding of Biomolecules. *Nat. Biotechnol.* **2001**, *19* (7), 631−635.
(19) Lu, Y.; Lu, J.; Zhao, J.; Cusido, J.; Raymo, F. M.; Yuan, J.; Yang, S.; Leif, R. C.; et al. On-the-Fly Decoding Luminescence Lifetimes in the Microsecond Region for Lanthanide-Encoded Suspension Arrays. *Nat. Commun.* **2014**, *5* (1), 3741.
(20) Zhou, L.; Fan, Y.; Wang, R.; Li, X.; Fan, L.; Zhang, F. High-capacity Upconversion Wavelength and Lifetime Binary Encoding for Multiplexed Biodetection. *Angew. Chem.* **2018**, *130* (39), 13006−13011.
(21) Dong, H.; Sun, L. D.; Feng, W.; Gu, Y.; Li, F.; Yan, C. H. Versatile Spectral and Lifetime Multiplexing Nanoplatform with Excitation Orthogonalized Upconversion Luminescence. *ACS Nano* **2017**, *11* (3), 3289−3297.
(22) Shen, J.; Xu, B.; Wang, Z.; Zhang, J.; Zhang, W.; Gao, Z.; Wang, X.; Zhu, C.; Meng, X. Aggregation-Induced Room Temperature Phosphorescent Carbonized Polymer Dots with Wide-Range Tunable Lifetimes for Optical Multiplexing. *J. Mater. Chem. C* **2021**, *9* (21), 6781−6788.
(23) Ou, Y.; Zhou, W.; Zhu, Z.; Ma, F.; Zhou, R.; Su, F.; Zheng, L.; Ma, L.; Liang, H. Host Differential Sensitization toward Color/Lifetime-Tuned Lanthanide Coordination Polymers for Optical Multiplexing. *Angew. Chem.* **2020**, *132* (52), 24018−24024.
(24) Mizuno, T.; Hase, E.; Minamikawa, T.; Tokizane, Y.; Oe, R.; Koresawa, H.; Yamamoto, H.; Yasui, T. Full-Field Fluorescence Lifetime Dual-Comb Microscopy Using Spectral Mapping and Frequency Multiplexing of Dual-Comb Optical Beats. *Sci. Adv.* **2021**, *7* (1), 1−12.
(25) Ortgies, D. H.; Tan, M.; Ximendes, E. C.; Del Rosal, B.; Hu, J.; Xu, L.; Wang, X.; Martín Rodríguez, E.; Jacinto, C.; Fernandez, N.; Chen, G.; Jaque, D. Lifetime-Encoded Infrared-Emitting Nanoparticles for in Vivo Multiplexed Imaging. *ACS Nano* **2018**, *12* (5), 4362−4368.
(26) Wu, S.; Han, G.; Milliron, D. J.; Aloni, S.; Altoe, V.; Talapin, D. V.; Cohen, B. E.; Schuck, P. J. Non-Blinking and Photostable Upconverted Luminescence from Single Lanthanide-Doped Nanocrystals. *Proc. Natl. Acad. Sci. U. S. A.* **2009**, *106* (27), 10917−10921.
(27) Xu, J.; Zhou, J.; Chen, Y.; Yang, P.; Lin, J. Lanthanide-Activated Nanoconstructs for Optical Multiplexing. *Coord. Chem. Rev.* **2020**, *415*, 213328.
(28) Liu, X.; Wang, Y.; Li, X.; Yi, Z.; Deng, R.; Liang, L.; Xie, X.; Loong, D. T. B.; Song, S.; Fan, D. Binary Temporal Upconversion Codes of Mn^{2+}-Activated Nanoparticles for Multilevel Anti-Counterfeiting. *Nat. Commun.* **2017**, *8* (1), 1−7.
(29) Lu, Y.; Zhao, J.; Zhang, R.; Liu, Y.; Liu, D.; Goldys, E. M.; Yang, X.; Xi, P.; Sunna, A.; Lu, J.; Shi, Y.; Leif, R. C.; Huo, Y.; Shen, J.; Piper, J. A.; Robinson, J. P.; Jin, D. Tunable Lifetime Multiplexing Using Luminescent Nanocrystals. *Nat. Photonics* **2014**, *8* (1), 32−36.
(30) Liao, J.; Zhou, J.; Song, Y.; Liu, B.; Chen, Y.; Wang, F.; Chen, C.; Lin, J.; Chen, X.; Lu, J.; Jin, D. Preselectable Optical Fingerprints of Heterogeneous Upconversion Nanoparticles. *Nano Lett.* **2021**, *21* (18), 7659−7668.
(31) Gómez-Bombarelli, R.; Aguilera-Iparraguirre, J.; Hirzel, T. D.; Duvenaud, D.; Maclaurin, D.; Blood-Forsythe, M. A.; Chae, H. S.; Einzinger, M.; Ha, D. G.; Wu, T.; et al. A Design of Efficient Molecular Organic Light-Emitting Diodes by a High-Throughput Virtual Screening and Experimental Approach. *Nat. Mater.* **2016**, *15* (10), 1120−1127.
(32) Carrasquilla, J.; Melko, R. G. Machine Learning Phases of Matter. *Nat. Phys.* **2017**, *13* (5), 431−434.
(33) De Albuquerque, V. H. C.; Cortez, P. C.; De Alexandria, A. R.; Tavares, J. M. R. S. A New Solution for Automatic Microstructures Analysis from Images Based on a Backpropagation Artificial Neural Network. *Nondestr. Test. Eval.* **2008**, *23* (4), 273−283.
(34) Kalinin, S. V.; Sumpter, B. G.; Archibald, R. K. Big-Deep-Smart Data in Imaging for Guiding Materials Design. *Nat. Mater.* **2015**, *14* (10), 973−980.
(35) Greenaway, R. L.; Santolini, V.; Bennison, M. J.; Alston, B. M.; Pugh, C. J.; Little, M. A.; Miklitz, M.; Eden-Rump, E. G. B.; Clowes, R.; Shakil, A.; Cuthbertson, H. J.; Armstrong, H.; Briggs, M. E.; Jelfs, K. E.; Cooper, A. I. High-Throughput Discovery of Organic Cages and Catenanes Using Computational Screening Fused with Robotic Synthesis. *Nat. Commun.* **2018**, *9* (1), 2849.
(36) Granda, J. M.; Donina, L.; Dragone, V.; Long, D. L.; Cronin, L. Controlling an Organic Synthesis Robot with Machine Learning to Search for New Reactivity. *Nature* **2018**, *559* (7714), 377−381.
(37) Penumuru, D. P.; Muthuswamy, S.; Karumbu, P. Identification and Classification of Materials Using Machine Vision and Machine Learning in the Context of Industry 4.0. *J. Intell. Manuf.* **2020**, *31* (5), 1229−1241.
(38) Madiona, R. M. T.; Winkler, D. A.; Muir, B. W.; Pigram, P. J. Optimal Machine Learning Models for Robust Materials Classification Using ToF-SIMS Data. *Appl. Surf. Sci.* **2019**, *487*, 773−783.

https://doi.org/10.1021/acs.jpclett.1c02923
J. Phys. Chem. Lett. 2021, 12, 10242−10248

(39) Zhou, Q.; Tang, P.; Liu, S.; Pan, J.; Yan, Q.; Zhang, S. C. Learning Atoms for Materials Discovery. *Proc. Natl. Acad. Sci. U. S. A.* **2018**, *115* (28), E6411−E6417.
(40) Raccuglia, P.; Elbert, K. C.; Adler, P. D. F.; Falk, C.; Wenny, M. B.; Mollo, A.; Zeller, M.; Friedler, S. A.; Schrier, J.; Norquist, A. J. Machine-Learning-Assisted Materials Discovery Using Failed Experiments. *Nature* **2016**, *533* (7601), 73−76.
(41) Schütt, K. T.; Glawe, H.; Brockherde, F.; Sanna, A.; Müller, K. R.; Gross, E. K. U. How to Represent Crystal Structures for Machine Learning: Towards Fast Prediction of Electronic Properties. *Phys. Rev. B: Condens. Matter Mater. Phys.* **2014**, *89* (20), 1−5.
(42) Carr, D. A.; Lach-Hab, M.; Yang, S.; Vaisman, I. I.; Blaisten-Barojas, E. Machine Learning Approach for Structure-Based Zeolite Classification. *Microporous Mesoporous Mater.* **2009**, *117* (1−2), 339−349.
(43) Ho, C.-S.; Jean, N.; Hogan, C. A.; Blackmon, L.; Jeffrey, S. S.; Holodniy, M.; Banaei, N.; Saleh, A. A. E.; Ermon, S.; Dionne, J. Rapid Identification of Pathogenic Bacteria Using Raman Spectroscopy and Deep Learning. *Nat. Commun.* **2019**, *10* (1), 1−8.
(44) Medina-Ortiz, D.; Contreras, S.; Quiroz, C.; Olivera-Nappa, Á. Development of Supervised Learning Predictive Models for Highly Non-Linear Biological, Biomedical, and General Datasets. *Front. Mol. Biosci.* **2020**, *7*, 13.
(45) Wiecha, P. R.; Lecestre, A.; Mallet, N.; Larrieu, G. Pushing the Limits of Optical Information Storage Using Deep Learning. *Nat. Nanotechnol.* **2019**, *14* (3), 237−244.
(46) Kiarashinejad, Y.; Abdollahramezani, S.; Zandehshahvar, M.; Hemmatyar, O.; Adibi, A. Deep Learning Reveals Underlying Physics of Light-Matter Interactions in Nanophotonic Devices. *Adv. Theory Simulations* **2019**, *2* (9), 1−9.

https://doi.org/10.1021/acs.jpclett.1c02923
J. Phys. Chem. Lett. 2021, 12, 10242−10248